



Bidirectional Edge-Resonant Switched Capacitor Cell-Assisted Soft-Switching Dc-Dc Converter

Saritha Thomas Vaidyan¹, Rabiya Rasheed²

Student, Dept. of EEE, FISAT, Angamaly, Ernakulam, Kerala, India¹

Assistant Professor, Dept. of EEE, FISAT, Angamaly, Ernakulam, Kerala, India²

ABSTRACT: Here a soft-switching pulse width modulation (PWM) non-isolated bidirectional dc-dc (BDC) converter embedding an edge-resonant switched capacitor (ER-SWC) cell is presented. Bidirectional dc-dc converters serve the purpose of stepping up or stepping down the voltage level between its input and output. Bidirectional dc-dc converter has the capability of power flow in both the directions. The conceptual bidirectional dc-dc converter treated here can be operated in two modes: - buck mode (step-down) operation and boost mode (step-up) operation. The converter here operated in discontinuous conduction mode (DCM). So the converter can achieve high-frequency zero-current soft-switching (ZCS) turn-on and zero-voltage soft-switching (ZVS) turn-off operations in the active switches. Those advantageous properties enable a wide range of soft-switching operations together with a high-voltage step-up conversion ratio with a reduced current stress. Circuit design guidelines based on the soft-switching range is introduced. Then, a theoretical analysis is carried out for investigating the step-up voltage conversion ratio. The simulation is carried out here in MATLAB/Simulink platform. For demonstrating the effectiveness of the soft-switching PWM bidirectional dc-dc converter, a 22W-40kHz prototype is evaluated in experiments, and then its performances are discussed.

KEYWORDS: Bidirectional dc-dc converters, soft-switching, Edge-resonant, Discontinuous Conduction

I. INTRODUCTION

Bidirectional dc-dc converters (BDC) have recently received a lot of attention due to the increasing need to systems with the capability of bidirectional energy transfer between two dc buses. Apart from traditional application in dc motor drives, new applications of BDC include energy storage in renewable energy systems, fuel cell energy systems and uninterruptible power supplies (UPS). The fluctuation nature of most renewable energy resources, like wind and solar, makes them unsuitable for standalone operation as the sole source of power. A common solution to overcome this problem is to use an energy storage device besides the renewable energy resource to compensate for these fluctuations and maintain a smooth and continuous power flow to the load. As the most common and economical energy storage devices are batteries and super-capacitors. A dc-dc converter is always required to allow energy exchange between storage device and the rest of system. Such a converter must have bidirectional power flow capability with flexible control in all operating modes. To charge and discharge the storage element, the bidirectional DC-DC converter is used. Here a non-isolated bidirectional edge-resonant switched capacitor cell-assisted soft-switching dc-dc converter is presented. It is derived from an edge-resonant switched capacitor cell-assisted soft-switching PWM boost dc-dc converter [1]. The bidirectional converter can be operated in two modes: buck mode and boost mode. Edge resonance means resonance occurs at rising or falling edge of the PWM signal. The converter is operating in discontinuous conduction mode. By adopting discontinuous conduction mode (DCM) scheme, the conventional PWM boost dc-dc converter can attain the soft commutation naturally at the turn-on of the active switch and zero-current soft-switching (ZCS) turn-off of the freewheeling diode in the wide range of load variation without any additional circuit component. Those advantages lead to the simplicity in the main circuit configuration and the control systems.

However, there exists an inherent technical issue in the DCM scheme: the current stress in the power devices and components as well as in the input smoothing capacitor is larger than that of the PWM boost dc-dc converter in CCM. To overcoming the drawbacks of the PWM boost dc-dc converter in DCM, employment of the edge-resonant switched capacitor (ER-SWC) cell [13] is one of the effective techniques due to its high efficiency and high scalability characteristics. In the soft-switching PWM boost dc-dc converter with the ER-SWC cell, a wide range of soft-switching operations can be achieved under the condition of DCM/critical conduction mode (CRM) in the input dc current without any circulating current, while the current stresses in the power devices and the passive components can also be mitigated owing to the edge resonance within the switching cell.

II. PROPOSED TOPOLOGY

The modified converter is a bidirectional edge-resonant switched capacitor cell-assisted soft-switching PWM dc-dc converter. The circuit configuration of the bidirectional ER-SWC soft-switching PWM dc-dc converter shown in Fig.1

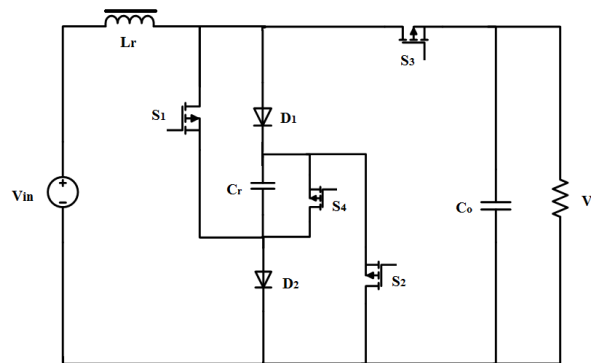


Fig 1: Circuit diagram of Proposed converter

The ER-SWC cell consists of four active switches S_1, S_2, S_3 and S_4 , two diodes D_1 and D_2 , a resonant capacitor C_r , and a resonant inductor L_r . This converter can work in two modes of operation i.e. in buck mode or in boost mode. When the switches S_1 and S_2 are on, the converter act as a boost converter. At that time S_3 and S_4 are off. In buck mode S_3 and S_4 , are operated. During that time S_1 and S_2 are off. Edge resonance means resonance occurs at the rising or falling edge of the PWM signal. The modified converter is an edge-resonant soft-switching converter, that means soft-switching happens at the rising or falling edge of the gate pulse

III. OPERATION PRINCIPLE

A. Boost mode

In this mode the dc-dc converter acts as a boost converter. The gate pulse is given to S_1 and S_2 , keeping S_3 and S_4 off. The mode transitions with the simplified equivalent circuits are shown in Fig.2. The circuit operation during one switching cycle is divided into five sub modes, as described in the following.

- Mode 1 [$t_0 \leq t < t_1$], (S_1, S_2 , ZCS turn-on mode): The inductor current i_{Lr} , is zero, and the active switches S_1 , and S_2 , are simultaneously turned ON at t_0 . Then, i_{Lr} and the switch currents i_{S1} and i_{S2} rise gradually from the zero initial value with the edge resonance by L_r and C_r . Thereby, ZCS turn-on commutation can be achieved in S_1 and S_2 . During this mode, i_{Lr} is written as

$$i_{Lr}(t) = \frac{V_{in} + V_0}{Z} \sin(\omega_r t - t_0) \quad (1)$$

where $Z = \sqrt{L_r / C_r}$ and $\omega_r = 1 / \sqrt{L_r C_r}$

The resonant capacitor C_r is discharged by i_{Lr} in this interval.

- Mode 2 [$t_1 \leq t < t_2$], (inductive energy storing mode): The resonant capacitor C_r is completely discharged at t_1 ; then, the diodes D_1 and D_2 are forward-biased. The beginning time t_1 of this sub mode and its inductor current i_{Lr1} can be determined from (1) as

$$t_1 = t_0 + \frac{1}{\omega_r} \cdot \cos^{-1} \left(\frac{V_{in}}{V_{in} + V_0} \right) \quad (2)$$

International Journal of Advanced Research in Electrical, Electronics and Instrumentation Engineering

(An ISO 3297: 2007 Certified Organization)

Vol. 3, Special Issue 5, December 2014

$$i_{Lr1} = i_{Lr}(t_1) = \frac{\sqrt{V_0(2V_{in} + V_0)}}{Z} \quad (3)$$

During this interval, i_{Lr} rises linearly as expressed by

$$i_{Lr}(t) = \frac{V_{in}}{L_r}(t - t_1) + I_{Lr1} \quad (4)$$

The inductor current I_{Lr} is equally shared by the two branches S_1-D_1 and S_2-D_2 .

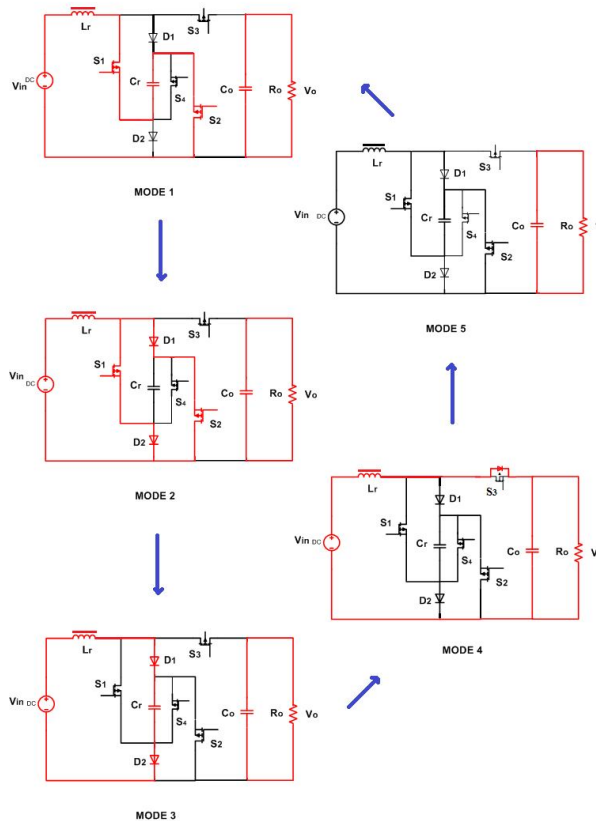


Fig 2. Operating modes during Boost operation

- Mode 3 [$t_2 \leq t < t_3$], (S_1, S_2 ZVS turn-off mode): The two active switches S_1 and S_2 are turned OFF simultaneously at t_2 . Then, the edge resonance begins again in the ER-SWC cell, and the voltages across S_1 and S_2 increase gradually by the effect of C_r . Thereby, ZVS turn-off commutation can be achieved in S_1 and S_2 . The inductor current i_{Lr2} at t_2 can be defined from (4) as

$$I_{Lr2} = i_{Lr}(t_2) = \frac{V_{in}}{L_r}(t_2 - t_1) + I_{Lr1} \quad (5)$$

where $t_2 = t_o + DT$ and D denotes the duty cycle of S_1 and S_2 as defined by

$$D \approx \frac{T_{on}}{T} \quad (6)$$

During this mode, i_{Lr} is defined by

$$I_{Lr}(t) = I_{max} \sin \left[\omega_r (t - t_2) + \tan^{-1} \left(\frac{Z I_{Lr2}}{V_{in}} \right) \right] \quad (7)$$

where I_{max} represents the peak value of i_{Lr} , as expressed by

$$I_{max} = \sqrt{I_{Lr2}^2 + \left(\frac{V_{in}}{Z} \right)^2} \quad (8)$$

This operation mode continues until the capacitor voltage V_{Cr} equals the output voltage V_o at t_3 .

International Journal of Advanced Research in Electrical, Electronics and Instrumentation Engineering

(An ISO 3297: 2007 Certified Organization)

Vol. 3, Special Issue 5, December 2014

- Mode 4 [$t_3 \leq t < t_4$], (*inductor energy releasing mode*): The resonant capacitor voltage V_{Cr} rises up to the output voltage at t_3 ; then, the conduction interval of D_1 and D_2 is terminated. The beginning time t_3 of the submode and the corresponding inductor current i_{Lr3} can be defined from (7) as

$$t_3 = t_2 + \frac{1}{\omega_r} \left\{ \sin^{-1} \left(\frac{V_o - V_{in}}{Z I_{max}} \right) + \tan^{-1} \left(\frac{V_{in}}{Z I_{Lr2}} \right) \right\} \quad (9)$$

$$i_{Lr3} = i_{Lr}(t_3) = \sqrt{I_{max}^2 - \left(\frac{V_o - V_{in}}{Z} \right)^2} \quad (10)$$

The inductor current i_{Lr} is forward to the load via D_o and thereby, the input voltage V_{in} is boosted to the output voltage V_o . During this interval, i_{Lr} is expressed by

$$i_{Lr}(t) = \frac{V_{in} - V_o}{L_r} (t - t_3) + I_{Lr3} \quad (11)$$

The inductor current i_{Lr} gradually decreases and naturally reaches to the zero level at t_4 . Accordingly, occurrence of the reverse recovering current in the output freewheeling diode D_o can be mitigated.

- Mode 5 [$t_4 \leq t < t_5$], (*inductor current discontinuous Mode*): Inductor current i_{Lr} reduces to zero level after t_4 , which is determined from (11) by

$$t_4 = t_3 + \frac{L_r I_{Lr3}}{V_o - V_{in}} \quad (12)$$

The load current flows through the output capacitor C_o in this submode; then, the inductor current keeps the zero level until the next switching cycle starts at t_5 .

B. Buck mode

In this mode the dc-dc converter acts as a buck converter. The gate pulse is given to S_3 and S_4 , keeping S_1 and S_2 off. The gate pulse given to switch S_4 is complimentary of S_3 . The mode transitions with the simplified equivalent circuits are shown in Fig.3

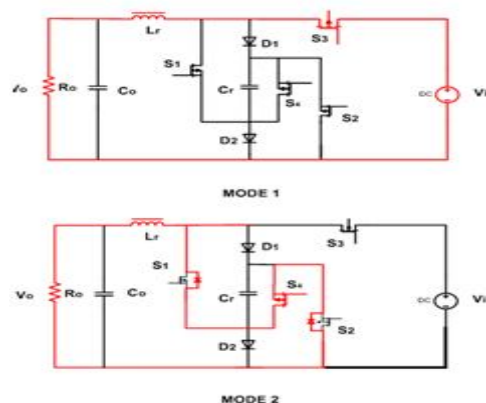


Fig 3. Operating modes during Boost operation

- Mode 1 [$0 \leq t < DT$], (S_3 on, S_4 off): During this interval S_3 is on, the ER-SWC cell is not conducting, because S_1, S_2 and S_4 are off and also D_1 and D_2 are reverse biased. The input provides energy to the load as well as to the inductor. The voltage across the inductor can be represented as

$$V_{Lr} = V_{in} - V_o \quad (13)$$

- Mode 2 [$DT \leq t < T$], (S_3 off, S_4 on): In this interval switch S_3 is off. The inductor discharges through load. The inductor current flows through L_r - R_o - S_2 - S_1

$$V_{Lr} = -V_o \quad (14)$$

IV. ANALYSIS OF VOLTAGE CONVERSION RATIO

The analysis of the bi-directional converter is done by considering its boost mode operation[1]. The inductor current and voltage waveforms of the ER-SWC soft-switching PWM dc–dc converter in boost mode are illustrated and compared with those of the conventional hard-switching PWM boost dc–dc converter in DCM under the condition of the same duty cycle in Fig.4. The positive voltage–second area S_B in fig.4

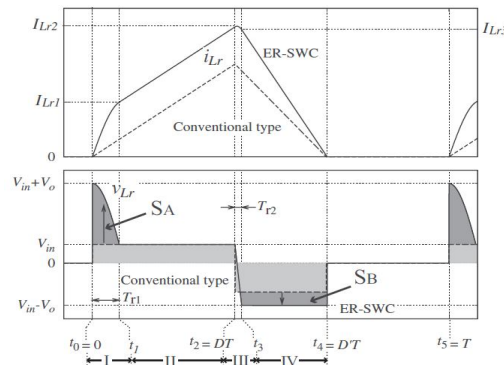


Fig 4:Current and voltage waveforms of input inductor L_r in DCM of conventional and ER-SWC dc–dc converters in boost mode under the same duty cycle condition.

As a result, the negative amplitude of V_{Lr} in Fig. 5 is extended much more than that of the conventional type, then a larger output voltage V_0 , i.e., higher voltage conversion ratio can be obtained in the ER-SWC dc–dc converter in boost mode. The voltage conversion ratio ($M = V_0/V_{in}$) of the ER-SWC boost dc–dc converter in DCM can be determined from the input and output power balance. By assuming the time origin $t_0 = 0$ in Fig. 5 for simplicity, the time integrations of the inductor current i_{Lr} in each submode are defined by

$$S_1 = \int_0^{t_1} i_{Lr} \cdot dt = C_r V_0 \tag{15}$$

$$S_2 = \int_{t_1}^{t_2} i_{Lr} \cdot dt = \frac{V_{in}}{2L_r} (DT - t_1)^2 + I_{Lr1} (DT - t_1) \tag{16}$$

$$S_3 = \int_{t_2}^{t_3} i_{Lr} \cdot dt = C_r V_0 \tag{17}$$

$$S_4 = \int_{t_3}^{t_4} i_{Lr} \cdot dt = \frac{L_r I_{Lr3}^2}{2(V_0 - V_{in})} \tag{18}$$

$$S_5 = \int_{t_4}^T i_{Lr} \cdot dt = 0 \tag{19}$$

Therefore, the average input current $\overline{i_{Lr}}$ can be obtained by

$$\overline{i_{Lr}} = \frac{1}{T} \int_0^T i_{Lr} \cdot dt = \frac{1}{T} \sum_{k=1}^5 S_k \tag{20}$$

Neglecting the power losses in the ER-SWC boost dc–dc converter, the power balances between the dc power source V_{in} and the load V_0 can be established as

$$V_{in} \overline{i_{Lr}} = \frac{V_0^2}{R_0} \tag{21}$$

The input power $V_{in} \overline{i_{Lr}}$ can be expressed from (15)–(21) as

$$V_{in} \overline{i_{Lr}} = \frac{V_{in} V_0}{T(V_0 - V_{in})} \left\{ \frac{V_{in}}{2L_r} (D_2 T)^2 + D_2 I_{Lr1} T + 2C_r V_0 \right\} \tag{22}$$

where $D_2 T = t_2 - t_1$. Furthermore, deformation of (21) with (22) yields the equation regarding the voltage conversion ratio M as

$$M^2 - (1 + 2C_r R_0 f_s) M - \frac{R_0 f_s}{Z_r} D_2 T (\sqrt{M^2 + 2M} - \frac{\omega_r}{2} D_2 T) = 0 \tag{23}$$

International Journal of Advanced Research in Electrical, Electronics and Instrumentation Engineering

(An ISO 3297: 2007 Certified Organization)

Vol. 3, Special Issue 5, December 2014

V. DESIGN GUIDELINE OF CIRCUIT PARAMETERS

The circuit parameters of L_r and C_r in the ER-SWC cell should be based on both of the maximum output power $P_{o,max}$ with the maximum duty cycle D_{max} and the minimum output power $P_{o,min}$ with the minimum duty cycle D_{min} . The determination of the zero crossing time of i_{Lr} , $t_4 = D_{max}T$, the maximum output power $P_{o,max}$ can be expressed as

$$P_{o,max} = V_{in} \overline{i_{Lr,max}} \quad (24)$$

Where $\overline{i_{Lr}}$ represents the average current of i_{Lr} at $P_o = P_{o,max}$ and this value can be obtained from (1), (4), (7), and (11); then, $i_{Lr,max}$ means its maximum value. Then, the minimum output power $P_{o,min}$ can be given by

$$P_{o,min} = V_{in} \overline{i_{Lr,min}} = \frac{2C_r V_{in} V_0}{T} \left(1 + \frac{V_{in}}{V_0 - V_{in}} \right) \quad (25)$$

where $\overline{i_{Lr,min}}$ denotes the minimum value of the resonant inductor average current $\overline{i_{Lr}}$. Deformation of (25) yields the parameter of the resonant capacitor C_r as expressed by

$$C_r = \frac{(\frac{V_0}{V_{in}} - 1) P_{o,min}}{2 f_s V_0^2} \quad (26)$$

The parameter of L_r should meet the condition indicated as follows

$$L_r \leq 1 / C_r f_s^2 \left\{ \sin^{-1} \left(\frac{M-1}{M+1} \right) + \frac{2\sqrt{M}}{M-1} + \frac{\pi}{2} \right\}^2 \quad (27)$$

VI. SIMULATION RESULTS

The software used for simulation is MATLAB/Simulink. The proposed converter has two modes of operation, Boost Mode and Buck mode. In boost mode gate pulse is given to S_1 and S_2 . Fig.5 shows the simulink model of the bidirectional converter during boost mode. In boost mode the input voltage is in the range of 30V-100V and output is obtained as 200V. In buck mode gate pulse is given to S_3 and S_4 . The gate pulse given to switch S_4 is complementary of switch S_3 . Fig.6 shows the simulink model of the bidirectional converter during buck mode. In buck mode 200V is given as input and 30V is obtained as output. The switching frequency is 40 kHz.

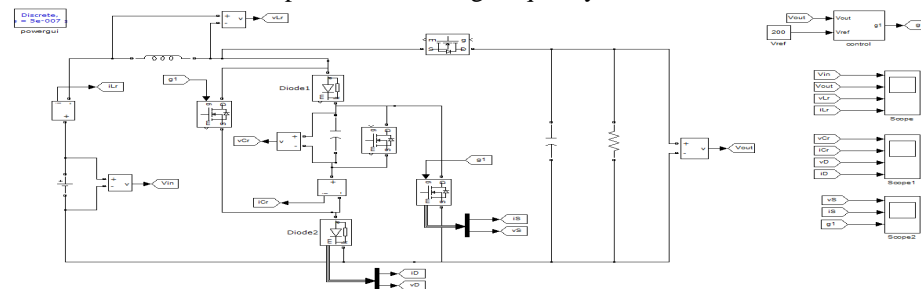


Fig.5 Simulink model of boost mode

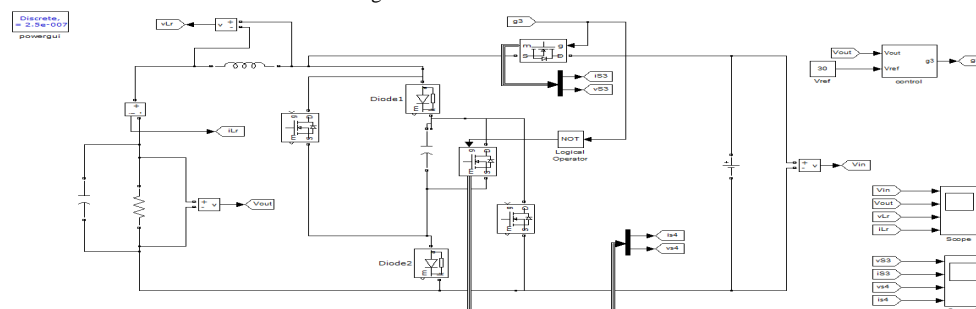


Fig.6 Simulink model of Buck Mode

International Journal of Advanced Research in Electrical, Electronics and Instrumentation Engineering

(An ISO 3297: 2007 Certified Organization)

Vol. 3, Special Issue 5, December 2014

Fig.7(a),(b) shows the input and output voltage waveforms during boost mode. Input voltage is 30V and output voltage is obtained as 200V.

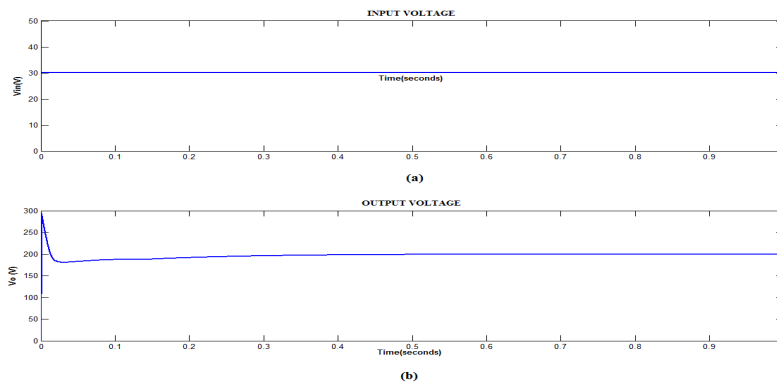


Fig.7 (a)Input Voltage (b) Output Voltage

Fig.8 (a),(b) shows the waveforms of input and output voltage during buck mode. Input voltage is 200V and output voltage is obtained as 30V.

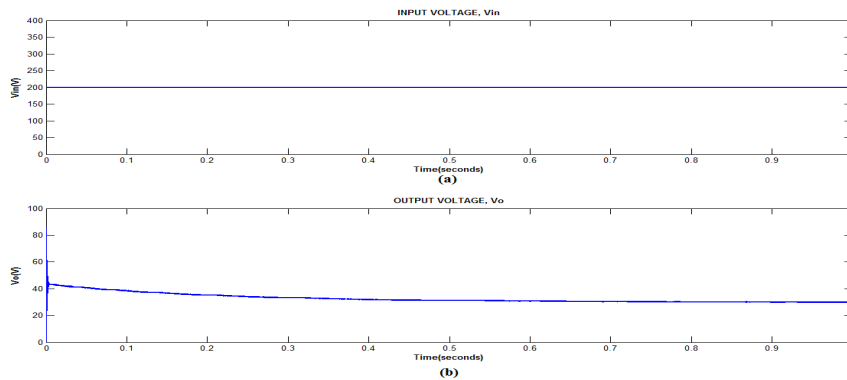


Fig.8 (a)Input Voltage (b) Output Voltage

Fig.9 shows the hardware implementation of the Bidirectional DC-DC converter

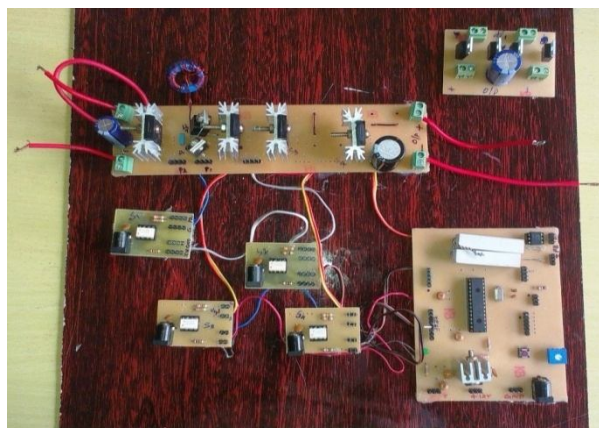


Fig.9 Hardware Implementation



International Journal of Advanced Research in Electrical, Electronics and Instrumentation Engineering

(An ISO 3297: 2007 Certified Organization)

Vol. 3, Special Issue 5, December 2014

VII. CONCLUSION

The Bi-Directional converter plays an important role in renewable energy applications. The proposed non-isolated bi-directional edge resonant switched capacitor cell assisted soft switching DC-DC converter can work in either boost mode or buck mode. This converter can achieve high-frequency zero-current soft-switching turn-on and zero-voltage soft-switching turn-off operations in the active switches. As a result a wide range of soft-switching operations together with a high-voltage step-up conversion ratio with a reduced current stress.

ACKNOWLEDGMENT

Initially, I would like to thank, the God Almighty for showing his blessings on me for successful completion of this work. Also I would like to thanks teachers, friends and parents.

REFERENCES

- [1] T. Mishima and M. Nakaoka, "Analysis, Design, and Performance Evaluations of an Edge-Resonant Switched Capacitor Cell-Assisted Soft-Switching PWM Boost DC-DC Converter and Its Interleaved Topology", IEEE Tran. Power Electron, VOL. 28, NO. 7, July 2013
- [2] Y. P. Hsieh, J. F. Chen, T. J. Liang, and L. S. Yang, "A novel high step-up DC-DC converter for a microgrid system," IEEE Trans. Power Electron., vol. 26, no. 4, pp. 1127–1136, Apr. 2011.
- [3] R. J. Wai and R. Y. Duan, "High step-up converter with coupled-inductor," IEEE Trans. Power Electron., vol. 20, no. 5, pp. 1025–1035, Sep. 2005.
- [4] E. C. Dias, L. C. G. Freitas, E. A. A. Coelho, J. B. Vieira, Jr., and L. C. de Freitas, "Novel true zero current turn-on and turn-off converters family: Analysis and experimental results," IET Power Electron., vol. 3, no. 1, pp. 33–42, 2010.
- [5] S. H. Park, G. R. Cha, Y. C. Jung, and C. Y. Won, "Design and application for PV generation system using a soft-switching boost converter with SARC," IEEE Trans. Ind. Electron., vol. 57, no. 2, pp. 515–522, Feb. 2010.
- [6] H.-L. Do, "A soft-switching DC/DC converter with high voltage gain," IEEE Trans. Power Electron., vol. 25, no. 5, pp. 1193–1200, May 2010
- [7] P. Das and G. Moschopoulos, "A comparative study of zero-current transition PWM converters," IEEE Trans. Ind. Electron., vol. 54, no. 3, pp. 1319–1328, Jun. 2007.
- [8] K.-H. Liu and F. C. Lee, "Zero-voltage switching technique in DC/DC converters," IEEE Trans. Power Electron., vol. 5, no. 3, pp. 293–304, Jul. 1990.
- [9] I. Aksoy, H. Bodur, and A. F. Bakan, "A new ZVT-ZCS-PWM dc-dc converter," IEEE Trans. Power Electron., vol. 25, no. 8, pp. 2093–2105, Aug. 2010.
- [10] C. M. Stein, J. Pinheiro, and H. L. Hey, "A ZCT auxiliary commutation circuit for interleaved boost converters operating in critical conduction mode," IEEE Trans. Power Electron., vol. 17, no. 6, pp. 954–961, Nov. 2002.
- [11] K. Yao, X. Ruan, X. Mao, and Z. Ye, "Reducing storage capacitor of a DCM boost PFC converter," IEEE Trans. Power. Electron., vol. 27, no. 1, pp. 151–160, Jan. 2012
- [12] K. Yao, X. Ruan, X. Mao, and Z. Ye, "Variable-duty-cycle control to achieve high input power factor for DCM boost PFC converter," IEEE Trans. Ind. Electron., vol. 58, no. 5, pp. 1856–1865, May 2011
- [13] T. Mishima and M. Nakaoka, "A new family of ZCS-PWM dc-dc converter with clamping diodes-assisted active edge-resonant cell," in Proc. Int. Conf. Electr. Mach. Syst., Oct. 2010, pp. 168–173